Spontaneous Formation of Star-Shaped Surface Patterns in a Driven Bose-Einstein Condensate

K. Kwon,[1] K. Mukherjee,[2] S. J. Huh,[1] K. Kim,[1] S. I. Mistakidis,[3] D. K. Maity,[2] P. G. Kevrekidis,[4] S. Majumder,[2] P. Schmelcher,[3,5] and J.-y. Choi[1,*]

[1]*Department of Physics, Korea Advanced Institute of Science and Technology, Daejeon 34141, Korea*
[2]*Department of Physics, Indian Institute of Technology Kharagpur, Kharagpur-721302, India*
[3]*Center for Optical Quantum Technologies, Department of Physics,University of Hamburg, Luruper Chaussee 149, 22761 Hamburg, Germany*
[4]*Department of Mathematics and Statistics, University of Massachusetts, Amherst, Massachusetts 01003-4515, USA*
[5]*The Hamburg Centre for Ultrafast Imaging, University of Hamburg, Luruper Chaussee 149, 22761 Hamburg, Germany*

(Received 20 May 2021; accepted 3 August 2021; published 10 September 2021)

We observe experimentally the spontaneous formation of star-shaped surface patterns in driven Bose-Einstein condensates. Two-dimensional star-shaped patterns with l-fold symmetry, ranging from quadrupole ($l = 2$) to heptagon modes ($l = 7$), are parametrically excited by modulating the scattering length near the Feshbach resonance. An effective Mathieu equation and Floquet analysis are utilized, relating the instability conditions to the dispersion of the surface modes in a trapped superfluid. Identifying the resonant frequencies of the patterns, we precisely measure the dispersion relation of the collective excitations. The oscillation amplitude of the surface excitations increases exponentially during the modulation. We find that only the $l = 6$ mode is unstable due to its emergent coupling with the dipole motion of the cloud. Our experimental results are in excellent agreement with the mean-field framework. Our work opens a new pathway for generating higher-lying collective excitations with applications, such as the probing of exotic properties of quantum fluids and providing a generation mechanism of quantum turbulence.

DOI: 10.1103/PhysRevLett.127.113001

Introduction.—Spontaneous pattern formation is frequently encountered in various research fields, including chemistry, biology, nonlinear optics, and cosmology [1–3]. Faraday waves constitute one of the earliest and most celebrated examples thereof that can be observed when a fluid in a vessel is subject to a vertical periodic modulation [4]. The underlying mechanism of these phenomena is the existence of instabilities, manifested in the related nonlinear hydrodynamic equations. The instabilities characterize a dominant wavelength that breaks the spatial and temporal symmetries of the system [1]. This has applications in measuring the intrinsic properties of fluids like density and surface tension [5,6]. Moreover, recent experiments with tracer particles in the Faraday waves have revealed the emergence of two-dimensional (2D) turbulence [7–9] and self-organization of flows with various patterns [10], thus extending the research scope of parametrically driven systems.

Bose-Einstein condensates (BECs) of atomic gases offer a fertile platform for transferring the relevant knowledge of nonlinear dynamics in classical settings to the realm of quantum many-body systems [11–16]. One-dimensional Faraday waves have been indeed observed in BECs under the periodic modulation of the transverse trap frequency of an elongated condensate [11] or of the s-wave scattering length near the magnetic Feshbach resonance [12]. Increasing the modulation strength with low driving frequency, irregular patterns (granulation) are generated characterized by fairly sizable quantum fluctuations [12], and bearing features of quantum turbulence [17]. However, the majority of experimental efforts has been performed in one dimension [11,12]. As such, various correlation patterns emerging from nonlinear wave mixing [13], surface excitations either from parametrically driven multicomponent systems [18] or from quantum fluctuations, such as quantum capillary waves in optical lattices [19], and the relation of Faraday waves to turbulent behavior in higher dimensions [16,20] are yet a largely unexplored territory.

In this Letter, we report the controlled generation of surface modes of different wavenumbers in atomic quantum fluids. Specifically, 2D regular polygons exhibiting an l-fold symmetry (from $l = 2$ to $l = 7$) develop from radially symmetric condensates by modulating the atomic interactions near the Feshbach resonance. The observed surface patterns have no preferred orientation and oscillate sinusoidally according to the modulation frequency. The associated spatial and temporal symmetry breaking phenomenon can be understood in terms of the hydrodynamic (parametric) instability, where an effective Mathieu equation describes the stability boundaries of the individual patterns. Probing the instability regions, we accurately measure the dispersion relation of the surface modes of

the harmonically trapped superfluid. The experimental results show an excellent agreement with the predictions of the three-dimensional (3D) mean-field Gross-Pitaevskii equation (GPE), demonstrating that BECs represent an ideal platform to emulate a number of classical fluid phenomena. Our findings should be valuable in conducting future experiments to measure several fundamental properties such as surface tension in quantum fluids [18] and to estimate the dynamical response through structure formation [21]. Additionally, they should assist in quantifying the generation of quantum turbulence and in enabling the realization of discrete-time crystals [22,23].

Experimental and theoretical setup.—The experiment is initiated by producing a BEC of ^{7}Li atoms in the $|F = 1, m_F = 1\rangle$ state near the Feshbach resonance [24]. The scattering length is set to $a_{bg} = 138(6)a_B$ (a_B is the Bohr radius). The condensate resides in a highly anisotropic harmonic trap consisting of a tight confining optical trap in the axial direction [25] and a weak magnetic trap constituting the radially symmetric confinement [Fig. 1(a)]. The trap frequencies are measured to be $[\omega_r, \omega_z] = 2\pi \times [29.4(2), 725(5)]$ Hz. Then, we apply a sinusoidally oscillating magnetic field to the pancake-shaped condensate, which modulates the scattering length $a_s(t)$ of the atoms [Fig. 1(a)]. Following a modulation time t, we take *in situ* absorption images under the Feshbach magnetic field and measure the atomic density distribution.

After 1 s of modulation, the condensate boundary is strongly deformed, displaying 2D regular polygon patterns along the xy plane [Figs. 1(b)–1(g)]. The generation of the surface modes is mostly driven by the scattering length modulation as the oscillation amplitude of the radial trap frequency is very weak (or insignificant), i.e., of about 0.3%. Moreover, the regular polygons show no preferred orientation in the horizontal plane, manifesting the spatio-temporal symmetry breaking phenomenon [Fig. 1(h)].

These surface modes are equally reproduced within the full 3D GPE framework [Figs. 1(i)–1(j)] which reads

$$i\hbar\frac{\partial}{\partial t}\Psi(x,y,z,t) = \left(-\frac{\hbar^2}{2m}\nabla_{\mathbf{r}}^2 + \frac{1}{2}m\omega_r^2(x^2+y^2+\lambda^2 z^2) + \frac{4\pi\hbar^2 a_s(t)}{m}|\Psi|^2\right)\Psi(x,y,z,t), \quad (1)$$

where $\int \mathbf{dr}|\Psi|^2 = N$ and $\nabla_{\mathbf{r}}^2 \equiv \partial_x^2 + \partial_y^2 + \partial_z^2$. Also, m and $\lambda = \omega_z/\omega_r$ represent the atomic mass and the aspect ratio of the trap. To emulate the thermal fraction in the present experiment (less than 10%), we consider a weak amplitude perturbation to the ground state, $\Psi_G(x,y,z)$, of the BEC. The initial wave function $\Psi_{\text{in}}(x,y,z) = \Psi_G(x,y,z)[1 + \varepsilon\delta(x,y,z)]$ [26,27]. Here, $\delta(x,y,z)$ is a Gaussian random distribution having zero mean and variance unity produced by using the so-called Box-Mueller algorithm [26,28] and $\varepsilon \ll 1$ mimics the thermal fraction being, herein, of the order of $\varepsilon \sim 0.1$, see the Supplemental Material [29].

Subsequently, we let the system [described by Eq. (1)] evolve upon considering a periodic modulation of the

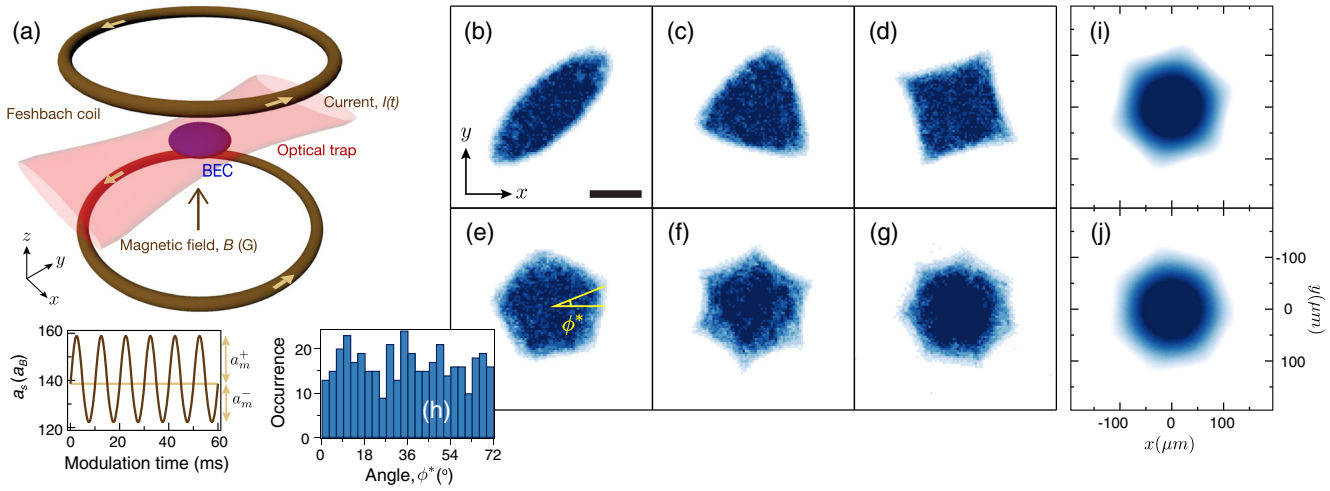

FIG. 1. Experimental observation of star-shaped condensates. (a) A BEC of ^{7}Li atoms is prepared in a pancake-shaped trap consisting of a red-detuned optical trap for the axial confinement and a magnetic trap, induced by Feshbach magnetic field curvature, for the radial confinement. The scattering length is modulated by oscillating the magnetic field near the Feshbach resonance. The mean modulation amplitude $\bar{a}_m$ is defined as the average of upper (a_m^+) and lower (a_m^-) modulation peaks, $\bar{a}_m = (a_m^+ + a_m^-)/2$. (b)–(g) Representative in trap images (single shots) of the ensuing regular polygons with D_l symmetry triggered by the periodic modulation. The modulation frequencies are 84 Hz (D_2), 104 Hz (D_3), 119 Hz (D_4), 132 Hz (D_5), 147 Hz (D_6), and 161 Hz (D_7), respectively. The mean modulation amplitude $\bar{a}_m = 19a_B$ ($a_m^+ = 21a_B$ and $a_m^- = 17a_B$). The scale bar in the $l = 2$ mode represents 100 μm. (h) The orientation angle ϕ^* for pentagon-shaped BECs, defined in (e), is measured with 400 consecutive experimental runs. The histogram displays the corresponding occurrence of the angle with bin size of 3°. (i) Hexagon and (j) heptagon-shaped patterns obtained by solving the 3D GPE (see main text).

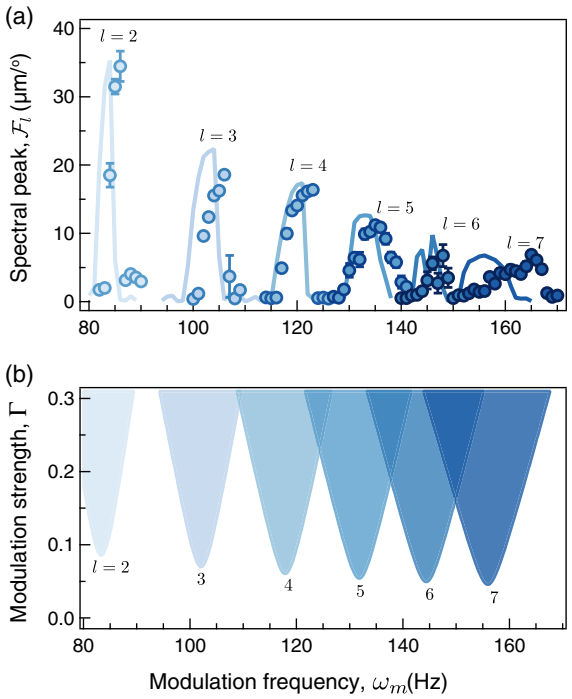

FIG. 2. Hydrodynamic instability of the surface excitations. (a) Spectral peak of various l-fold star patterns, created after 1 s of modulation, as a function of the modulation frequency. The spectral peak for the hexagon ($l = 6$ mode) is taken after $t = 0.3$ s due to the involved dipole instability (see main text). The filled circles designate the experimental results and solid lines refer to the GPE predictions; notice the very good agreement between the two. Each data point is averaged over 5–10 independent experimental realizations, and the error bars denote the standard deviation of the mean. (b) Floquet stability tongues for different modulation strengths $\bar{a}_m/a_{bg}$ and frequencies $\omega_m/(2\pi)$ characterizing distinct l-fold patterns.

scattering length of the form $a_s(t) = a_{bg} + \bar{a}_m \cos(\omega_m t)$, where $\bar{a}_m$ and ω_m are the mean modulation amplitude and frequency, dictated by the experiment. Figures 1(i) and 1(j) show characteristic density profiles, $n(x, y, t) = \int dz |\Psi(x, y, z, t)|^2$, of the D_6 and D_7 star patterns, respectively, obtained within the GPE framework. In the simulations, the surface modes are robust to the experimental imperfections, such as anisotropy in the radial confinement (∼3%), oscillations of the radial curvature (0.3%), and high harmonics in the scattering length modulation protocol.

Results and discussion.—To understand the underlying mechanism of the surface deformation, we study the frequency dependence of the surface modes at a fixed mean modulation amplitude $\bar{a}_m = 19a_B$. We characterize the polygon-shaped BECs with D_l symmetry, shown in Figs. 1(b)–1(g), by the Fourier amplitude $\mathcal{F}_l$ of the condensate radius over the azimuthal angle. The $\mathcal{F}_l$ quantifies the displacement of the condensate boundary with l-fold symmetry [29]. The D_l shaped BECs varying from ellipses ($l = 2$) to regular heptagons ($l = 7$) can be identified. Figure 2(a) displays the spectral peak $\mathcal{F}_l$ of each mode under various modulation frequencies. The surface modes ($l = 2$–7) are only excited at certain driving frequency intervals, in a way strongly reminiscent of the tongues in the Mathieu equation [48]. The resonance curves are asymmetric, resembling the response of a Duffing oscillator, which is well represented for $l \leq 4$ modes. When we reduce the modulation amplitude, the resonance spectra become more symmetric and acquire a narrower width [29], highlighting the role of nonlinear interactions during the surface deformation.

The onset of resonance behavior of the surface excitations can be unveiled by a Mathieu equation analysis for the amplitude of the density deformation, see details in Ref. [29]. Since the observed surface modes have no radial nodes, we assume a density disturbance of the form $\delta n = \zeta_l(t) r^l e^{il\phi}$. At short modulation times the deformation is small, and we arrive at the Mathieu equation for ζ_l after linearizing the hydrodynamic equations of the superfluid,

$$\ddot{\zeta}_l(t) + \omega_l^2 \left[1 + \frac{\bar{a}_m}{a_{bg}} \cos(\omega_m t)\right] \zeta_l(t) = 0, \tag{2}$$

where $\omega_l = \sqrt{l}\omega_r$. This equation represents a parametrically driven oscillator with a natural frequency ω_l, having a series of resonances at $\omega_m = 2\omega_l/n$, where n is an integer.

Within Floquet theory, a solution $\zeta_l(t) = e^{(s+i\alpha\omega_m)t} \sum_{k=-\infty}^{\infty} \zeta_l^{(k)} e^{ik\omega_m t}$ is sought, where s is its growth rate and α is the Floquet exponent [49]. For $s > 0$ the system is dynamically unstable and pattern formation takes place at the surface. Setting $s = 0$, we provide the marginal stability boundaries of the D_l symmetric patterns in Fig. 2(b). The stability diagram is composed of a series of resonant tongues, where the system exhibits star-shaped patterns if $\bar{a}_m$ and ω_m reside inside or at the boundaries of a specific tongue. Otherwise, the BEC cloud solely performs a collective breathing motion. The spectrum in Fig. 2(a) can be interpreted as the intersection of the instability tongues at modulation strength $\Gamma = \bar{a}_m/a_{bg} \simeq 0.14$.

Notice the not only qualitative but also quantitative match of the instability tongues between theoretical analysis, numerical findings, and experimental results and the weak deviation of the latter two when the nonlinear effects become more prominent as discussed above. Including a dissipative term $\gamma\dot{\zeta}_l$ to Eq. (2) lifts the tongues, suppressing pattern formation under a threshold amplitude. The dissipation rate $\gamma = 2\pi \times 1.8$ Hz, best matching the experimentally measured threshold amplitudes, is used. The temporal dynamics from the 3D GPE presents subharmonic oscillations $\omega_m/2$ of the surface modes, leading to the Floquet exponent $\alpha = 1/2$.

The theoretical investigations provide a deeper insight into the spontaneous pattern formation. The natural frequency ($\omega_l = \sqrt{l}\omega_r$) of the Mathieu equation is the dispersion of the surface excitation modes of superfluids

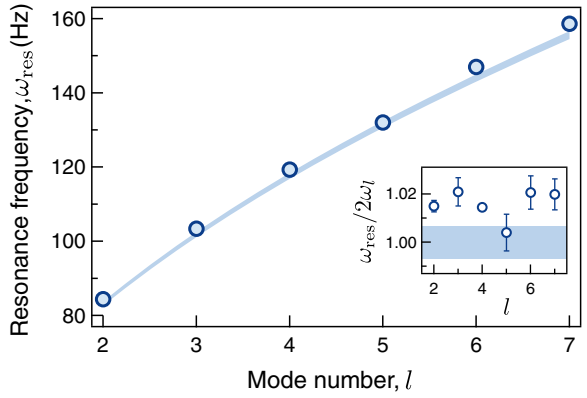

FIG. 3. Dispersion relation of the surface modes for superfluids in a harmonic trap. The spectral peak value for each l mode is obtained by fitting a Gaussian function to each resonance spectrum with small driving amplitude. Solid line represents a guide to the eye for the dispersion law of the surface mode in trapped superfluids. The inset shows the ratio of the measured resonance frequency and the hydrodynamic predictions. The error bars indicate a 95% confidence interval of the fit. Uncertainty of the radial trap frequency is marked by the shaded region.

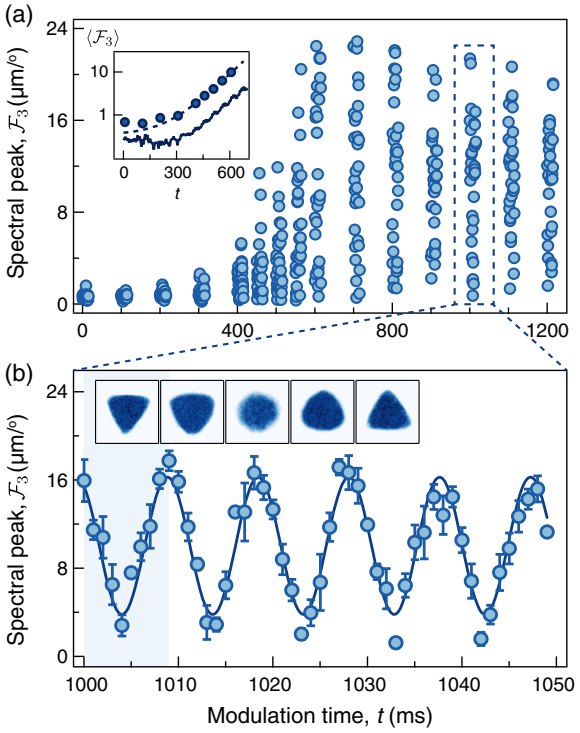

FIG. 4. Time evolution of the triangular surface mode. (a) Dynamics of the growth rate of the triangular mode under a 104 Hz modulation. The fluctuations of the spectral peak ($l = 3$) increase exponentially in the course of time. Each data point is a single experimental realization. Inset: the averaged spectral peak $\langle\mathcal{F}_3\rangle$ over a single oscillation time interval, $[t, t + 9.5]$ ms. Dashed line designates an exponential fit to the data (dark blue circle), and the solid line is obtained from the GPE simulation. (b) Zooming in at 1 s reveals the oscillation of the surface mode with 104 Hz driving frequency. Each data point corresponds to the mean over four independent experimental runs, and the error bars indicate the standard deviation of the mean. Inset: absorption images during the first oscillation period. The oscillation frequency is subharmonic, a result that is confirmed by the GPE calculations, see also Ref. [29].

in a harmonic potential [50]. It indicates that the observed star-shaped BECs subject to driving originate from the parametric excitation of the surface mode with high multipolarity. In other words, one can infer the dispersion laws by studying the resonance spectrum of each mode. To measure the resonance frequencies of the surface excitations, we investigate the surface mode spectrum with marginal mean modulation amplitude ($\bar{a}_m = 8$–$9a_B$) and sufficient condensate atom number [$N = 4.1(2) \times 10^6$]. Figure 3 depicts the measured resonance frequencies $\omega_{\rm res}(l)$ of different modes up to $l = 7$, which show a remarkable agreement with the predicted square-root scaling dispersion. Within the parameter regime that we operate, other effects from beyond mean-field [51], dipolar interactions [52], and finite particle number [29,50,51] are negligible. The observed small deviations (∼2%) might be attributed to the impact of the modulation on the resonance spectrum [29] and trap imperfections such as anharmonicity of the optical dipole trap [53].

Another characteristic feature of the parametric excitations is the exponential growth of the associated unstable modes as described by the solution of Eq. (2). Focusing on the $l = 3$ triangular mode, as a representative example of this phenomenology, we investigate the time evolution of the spectral peak $\mathcal{F}_3(t)$ at resonance driving $\omega_m = 2\pi \times 104$ Hz. Initially, small amplitude fluctuations of the condensate radius build up with no clear patterns, having $\mathcal{F}_3 \simeq 0$. After 300 ms of modulation, the azimuthal angular symmetry of the condensate boundary breaks, rapidly forming a regular triangle with sharp edges at $t = 600$ ms. Averaging the spectral peak within one period of oscillation $\langle\mathcal{F}_3\rangle$, we observe a clear manifestation of the parametric instability via the exponential growth dynamics [Fig. 4(a), inset], where the characteristic growth rate increases for higher l symmetry modes and driving amplitude [29].

As the evolution settles into a periodic pattern, the triangular surface mode undergoes a regular oscillation characterized by the external driving frequency [Fig. 4(b)]. The actual dynamics is subharmonic, a fact that is also confirmed within the GPE calculations. The peaks oscillate 90° out of phase with respect to the driving field, reflecting the dynamics of the Mathieu equation under resonant frequency driving. When turning off the periodic modulation after the development of the surface mode, the latter experiences a relaxation towards a symmetric shape. The dynamics follows a damped oscillatory motion, and the associated damping rate increases with the mode number and thermal fraction [54,55]; see details in [29]. We also note that higher-fold surface structures are created for increasing

$\omega_m/(2\pi)$, e.g., the D_{15} at $\omega_m/(2\pi) = 232$ Hz, while for $\omega_m/(2\pi) > 240$ Hz bulk patterns [21] in the form of star shapes and squarelike arrangements arise, see also [29].

Lastly, we would like to comment on the dynamics of the hexagon mode (D_6 pattern). Unlike the other surface excitations, this mode is found to be unstable due to its emergent coupling with the dipole motion of the cloud. This behavior is also found by the mean-field simulations. In the present study, we focus on the dispersion law of the surface modes, such that the resonance spectra in Fig. 2(a) and Fig. 3 are obtained for relatively short evolution times ($t \approx 300$ ms) and in particular before the dipole motion destabilizes the hexagonal pattern. Further details of the long-time dynamics of D_6 patterns are provided in Ref. [29]. This observation motivates further efforts to unveil possible signatures of turbulent properties of the surface modes.

Conclusions.—We observe experimentally and analyze theoretically the generation of star-shaped surface patterns in a BEC due to the Faraday wave instability induced by the periodic modulation of the scattering length. Quantitative monitoring of the patterns enables us to identify the growth rate of the parametric instability and to measure the dispersion relation of the surface excitations of superfluids in a harmonic trap, in very good agreement with theoretical predictions and numerical computations. Since our experimental method does not require special engineering to shape the condensates, it can be applied to various quantum fluids in a broad context, such as Fermi gases [53,56] and dipolar quantum fluids [57], as well as exciton-polariton BECs [58]. Moreover, relevant ideas extend to binary mixtures or quantum droplets, where the resonance spectrum can be utilized to extract the interfacial tension of the superfluid boundary [18]. By increasing the modulation strength, a transition to granulation and turbulent behavior, of interest in its own right [17], can be also studied in a two-dimensional condensate.

We acknowledge discussions with Jongchul Mun and thank Junhyeok Hur and Haejun Jung for critical reading of the manuscript. K. Kwon, S. J. Huh, K. Kim, and J.-y. Choi are supported by the Samsung Science and Technology Foundation BA1702-06 and National Research Foundation of Korea (NRF) Grant under Project No. 2020R1C1C1010863. K. Kim is supported by KAIST UP program. K. M. and D. K. M. acknowledge MHRD, Govt. of India for the research fellowship. S. I. M. gratefully acknowledges financial support in the framework of the Lenz-Ising Award of the University of Hamburg. This material is based upon work supported by the National Science Foundation under Grant No. PHY-2110030 and under Grant No. DMS-1809074 (P. G. K.).

*jae-yoon.choi@kaist.ac.kr

[1] M. C. Cross and P. C. Hohenberg, Pattern formation outside of equilibrium, Rev. Mod. Phys. **65**, 851 (1993).
[2] P. K. Maini, K. J. Painter, and H. N. Chau, Spatial pattern formation in chemical and biological systems, J. Chem. Soc., Faraday Trans. **93**, 3601 (1997).
[3] V. Petrov, Q. Ouyang, and H. L. Swinney, Resonant pattern formation in a chemical system, Nature (London) **388**, 655 (1997).
[4] M. Faraday, On a peculiar class of acoustical figures; and on certain forms assumed by groups of particles upon vibrating elastic surfaces, Phil. Trans. R. Soc. London **121**, 299 (1831).
[5] X. Noblin, A. Buguin, and F. Brochard-Wyart, Triplon Modes of Puddles, Phys. Rev. Lett. **94**, 166102 (2005).
[6] C. L. Shen, W. J. Xie, and B. Wei, Parametrically excited sectorial oscillation of liquid drops floating in ultrasound, Phys. Rev. E **81**, 046305 (2010).
[7] H. Xia, D. Byrne, G. Falkovich, and M. Shats, Upscale energy transfer in thick turbulent fluid layers, Nat. Phys. **7**, 321 (2011).
[8] A. von Kameke, F. Huhn, G. Fernández-García, A. P. Muñuzuri, and V. Pérez-Muñuzuri, Double Cascade Turbulence and Richardson Dispersion in a Horizontal Fluid Flow Induced by Faraday Waves, Phys. Rev. Lett. **107**, 074502 (2011).
[9] N. Francois, H. Xia, H. Punzmann, S. Ramsden, and M. Shats, Three-Dimensional Fluid Motion in Faraday Waves: Creation of Vorticity and Generation of Two-Dimensional Turbulence, Phys. Rev. X **4**, 021021 (2014).
[10] H. Alarcón, M. Herrera-Muñoz, N. Périnet, N. Mujica, P. Gutiérrez, and L. Gordillo, Faraday-Wave Contact-Line Shear Gradient Induces Streaming and Tracer Self-Organization: From Vortical to Hedgehoglike Patterns, Phys. Rev. Lett. **125**, 254505 (2020).
[11] P. Engels, C. Atherton, and M. A. Hoefer, Observation of Faraday Waves in a Bose-Einstein Condensate, Phys. Rev. Lett. **98**, 095301 (2007).
[12] J. H. V. Nguyen, M. C. Tsatsos, D. Luo, A. U. J. Lode, G. D. Telles, V. S. Bagnato, and R. G. Hulet, Parametric Excitation of a Bose-Einstein Condensate: From Faraday Waves to Granulation, Phys. Rev. X **9**, 011052 (2019).
[13] Z. Zhang, K.-X. Yao, L. Feng, J. Hu, and C. Chin, Pattern formation in a driven Bose–Einstein condensate, Nat. Phys. **16**, 652 (2020).
[14] M. Tsubota, M. Kobayashi, and H. Takeuchi, Quantum hydrodynamics, Phys. Rep. **522**, 191 (2013).
[15] P. G. Kevrekidis, D. J. Frantzeskakis, and R. Carretero-González, *The Defocusing Nonlinear Schrodinger Equation* (Society for Industrial and Applied Mathematics, Philadelphia, 2015).
[16] L. Madeira, M. Caracanhas, F. E. A. dos Santos, and V. S. Bagnato, Quantum Turbulence in Quantum Gases, Annu. Rev. Condens. Matter Phys. **11**, 37 (2020).
[17] A. U. J. Lode, M. C. Tsatsos, P. G. Kevrekidis, G. D. Telles, D. Luo, R. G. Hulet, and V. S. Bagnato, Onset and irreversibility of granulation of Bose-Einstein condensates under Feshbach resonance management, arXiv:2103.07479.
[18] D. K. Maity, K. Mukherjee, S. I. Mistakidis, S. Das, P. G. Kevrekidis, S. Majumder, and P. Schmelcher, Parametrically excited star-shaped patterns at the interface of binary Bose-Einstein condensates, Phys. Rev. A **102**, 033320 (2020).

[19] S. P. Rath, B. Spivak, and W. Zwerger, Quantum Capillary Waves at the Superfluid–Mott-Insulator Interface, Phys. Rev. Lett. **107**, 155703 (2011).

[20] J. A. Seman, E. A. L. Henn, R. F. Shiozaki, G. Roati, F. J. Poveda-Cuevas, K. M. F. Magalhães, V. I. Yukalov, M. Tsubota, M. Kobayashi, K. Kasamatsu, and V. S. Bagnato, Route to turbulence in a trapped Bose-Einstein condensate, Laser Phys. Lett. **8**, 691 (2011).

[21] K. Staliunas, S. Longhi, and G. J. de Valcárcel, Faraday Patterns in Bose-Einstein Condensates, Phys. Rev. Lett. **89**, 210406 (2002).

[22] J. Smits, L. Liao, H. T. C. Stoof, and P. van der Straten, Observation of a Space-Time Crystal in a Superfluid Quantum Gas, Phys. Rev. Lett. **121**, 185301 (2018).

[23] D. V. Else, C. Monroe, C. Nayak, and N. Y. Yao, Discrete time crystals, Annu. Rev. Condens. Matter Phys. **11**, 467 (2020).

[24] K. Kim, S. J. Huh, K. Kwon, and J.-y. Choi, Rapid production of large ^{7}Li Bose-Einstein condensates using D_1 gray molasses, Phys. Rev. A **99**, 053604 (2019).

[25] S. J. Huh, K. Kim, K. Kwon, and J.-y. Choi, Observation of a strongly ferromagnetic spinor Bose-Einstein condensate, Phys. Rev. Research **2**, 033471 (2020).

[26] H. Zheng, Y. Hao, and Q. Gu, Dynamics of double-well Bose–Einstein condensates subject to external Gaussian white noise, J. Phys. B **46**, 065301 (2013).

[27] N. P. Proukakis and B. Jackson, Finite-temperature models of Bose–Einstein condensation, J. Phys. B **41**, 203002 (2008).

[28] G. E. P. Box and M. E. Muller, A note on the generation of random normal deviates, Ann. Math. Stat. **29**, 610 (1958).

[29] See Supplemental Material at http://link.aps.org/supplemental/10.1103/PhysRevLett.127.113001 for the description of (1) Data analysis; (2) Dynamics of the patterns; (3) Details on the mean-field simulations; (4) Instability growth rate; (5) Mathieu equation and Floquet theory; (6) Finite-size effect; (7) Effect of the modulation amplitude and frequency; (8) Unstable dynamics of the D_6 pattern; and (9) Relaxation dynamics of the patterns, which includes Refs. [30–47].

[30] R. Saint-Jalm, P. C. M. Castilho, É. Le Cerf, B. Bakkali-Hassani, J.-L. Ville, S. Nascimbène, J. Beugnon, and J. Dalibard, Dynamical Symmetry and Breathers in a Two-Dimensional Bose Gas, Phys. Rev. X **9**, 021035 (2019).

[31] J. Crank and P. Nicolson, A practical method for numerical evaluation of solutions of partial differential equations of the heat-conduction type, Math. Proc. Cambridge Philos. Soc. **43**, 50 (1947).

[32] X. Antoine, W. Bao, and C. Besse, Computational methods for the dynamics of the nonlinear Schrödinger/Gross–Pitaevskii equations, Comput. Phys. Commun. **184**, 2621 (2013).

[33] D. F. Hill, The Faraday resonance of interfacial waves in weakly viscous fluids, Phys. Fluids **14**, 158 (2002).

[34] E. Madelung, Quantentheorie in hydrodynamischer form, Z. Phys. **40**, 322 (1927).

[35] C. Pethick and H. Smith, *Bose-Einstein Condensation of Dilute Gases* (Cambridge University Press, Cambridge, 2008).

[36] F. Dalfovo, S. Giorgini, M. Guilleumas, L. Pitaevskii, and S. Stringari, Collective and single-particle excitations of a trapped Bose gas, Phys. Rev. A **56**, 3840 (1997).

[37] R. J. A. Hill and L. Eaves, Vibrations of a diamagnetically levitated water droplet, Phys. Rev. E **81**, 056312 (2010).

[38] N. Goldman and J. Dalibard, Periodically Driven Quantum Systems: Effective Hamiltonians and Engineered Gauge Fields, Phys. Rev. X **4**, 031027 (2014).

[39] S. R. Barone, M. A. Narcowich, and F. J. Narcowich, Floquet theory and applications, Phys. Rev. A **15**, 1109 (1977).

[40] T. B. Benjamin, and F. J. Ursell, The stability of the plane free surface of a liquid in vertical periodic motion, Proc. Math. Phys. Eng. Sci. **225**, 505 (1954).

[41] K. Kumar, Linear theory of Faraday instability in viscous liquids, Proc. Math. Phys. Eng. Sci. **452**, 1113 (1996).

[42] P. G. Kevrekidis, W. Wang, R. Carretero-González, and D. J. Frantzeskakis, Adiabatic Invariant Approach to Transverse Instability: Landau Dynamics of Soliton Filaments, Phys. Rev. Lett. **118**, 244101 (2017).

[43] G. C. Katsimiga, S. I. Mistakidis, T. M. Bersano, M. K. H. Ome, S. M. Mossman, K. Mukherjee, P. Schmelcher, P. Engels, and P. G. Kevrekidis, Observation and analysis of multiple dark-antidark solitons in two-component Bose-Einstein condensates, Phys. Rev. A **102**, 023301 (2020).

[44] G. C. Katsimiga, S. I. Mistakidis, P. Schmelcher, and P. G. Kevrekidis, Phase diagram, stability and magnetic properties of nonlinear excitations in spinor Bose–Einstein condensates, New J. Phys. **23**, 013015 (2021).

[45] T. G. Skov, M. G. Skou, N. B. Jørgensen, and J. J. Arlt, Observation of a Lee-Huang-Yang Fluid, Phys. Rev. Lett. **126**, 230404 (2021).

[46] L. Pitaevskii and S. Stringari, Landau damping in dilute Bose gases, Phys. Lett. A **235**, 398 (1997).

[47] J. L. Ville, R. Saint-Jalm, É. Le Cerf, M. Aidelsburger, S. Nascimbène, J. Dalibard, and J. Beugnon, Sound Propagation in a Uniform Superfluid Two-Dimensional Bose Gas, Phys. Rev. Lett. **121**, 145301 (2018).

[48] I. Kovacic, R. Rand, and S. M. Sah, Mathieu's equation and its generalizations: Overview of stability charts and their features, Appl. Mech. Rev. **70**, 020802 (2018).

[49] A. Eckardt, Colloquium: Atomic quantum gases in periodically driven optical lattices, Rev. Mod. Phys. **89**, 011004 (2017).

[50] S. Stringari, Collective Excitations of a Trapped Bose-Condensed Gas, Phys. Rev. Lett. **77**, 2360 (1996).

[51] L. Pitaevskii and S. Stringari, Elementary Excitations in Trapped Bose-Einstein Condensed Gases Beyond the Mean-Field Approximation, Phys. Rev. Lett. **81**, 4541 (1998).

[52] S. E. Pollack, D. Dries, M. Junker, Y. P. Chen, T. A. Corcovilos, and R. G. Hulet, Extreme Tunability of Interactions in a ^{7}Li Bose-Einstein Condensate, Phys. Rev. Lett. **102**, 090402 (2009).

[53] M. Holten, L. Bayha, A. C. Klein, P. A. Murthy, P. M. Preiss, and S. Jochim, Anomalous Breaking of Scale Invariance in a Two-Dimensional Fermi Gas, Phys. Rev. Lett. **121**, 120401 (2018).

[54] P. O. Fedichev, G. V. Shlyapnikov, and J. T. M. Walraven, Damping of Low-Energy Excitations of a Trapped

Bose-Einstein Condensate at Finite Temperatures, Phys. Rev. Lett. **80**, 2269 (1998).

[55] R. Onofrio, D. S. Durfee, C. Raman, M. Köhl, C. E. Kuklewicz, and W. Ketterle, Surface Excitations of a Bose-Einstein Condensate, Phys. Rev. Lett. **84**, 810 (2000).

[56] A. Altmeyer, S. Riedl, C. Kohstall, M. J. Wright, R. Geursen, M. Bartenstein, C. Chin, J. H. Denschlag, and R. Grimm, Precision Measurements of Collective Oscillations in the BEC-BCS Crossover, Phys. Rev. Lett. **98**, 040401 (2007).

[57] L. Tanzi, S. M. Roccuzzo, E. Lucioni, F. Famà, A. Fioretti, C. Gabbanini, G. Modugno, A. Recati, and S. Stringari, Supersolid symmetry breaking from compressional oscillations in a dipolar quantum gas, Nature (London) **574**, 382 (2019).

[58] C. E. Whittaker, B. Dzurnak, O. A. Egorov, G. Buonaiuto, P. M. Walker, E. Cancellieri, D. M. Whittaker, E. Clarke, S. S. Gavrilov, M. S. Skolnick, and D. N. Krizhanovskii, Polariton Pattern Formation and Photon Statistics of the Associated Emission, Phys. Rev. X **7**, 031033 (2017).